IEEE Access
Multidisciplinary ⋮ Rapid Review ⋮ Open Access Journal

Received 1 May 2024, accepted 15 May 2024, date of publication 21 May 2024, date of current version 30 May 2024.

Digital Object Identifier 10.1109/ACCESS.2024.3403549

RESEARCH ARTICLE

Intelligent Multi-Group Marine Predator Algorithm With Deep Learning Assisted Anomaly Detection in Pedestrian Walkways

S. RAMA SREE [1], **E. LAXMI LYDIA** [2], **MOHAMMED ALTAF AHMED** [3], **K. RADHIKA** [4], **MOHAMAD KHAIRI ISHAK** [5], **KHALID AMMAR** [5], **(Member, IEEE), AND MOHAMED FAUZI PACKEER MOHAMED** [6]

[1]Department of CSE, Aditya Engineering College, Surampalem 533437, India
[2]Department of Computer Science and Engineering, GMR Institute of Technology, Rajam, Andhra Pradesh 532127, India
[3]Department of Computer Engineering, College of Computer Engineering and Science, Prince Sattam Bin Abdulaziz University, Al-Kharj 11942, Saudi Arabia
[4]AI and DS Department, Chaitanya Bharathi Institute of Technology, Hyderabad 500075, India
[5]Department of Electrical and Computer Engineering, College of Engineering and Information Technology, Ajman University, Ajman, United Arab Emirates
[6]School of Electrical and Electronic Engineering, Universiti Sains Malaysia, Nibong Tebal 14300, Malaysia

Corresponding author: Mohamad Khairi Ishak (m.ishak@ajman.ac.ae)

This work was supported in part by Ajman University, United Arab Emirates.

ABSTRACT Anomaly Detection (AD) in Pedestrian Walkways (PWs) is critical to urban security and safety systems. It is widely used to detect abnormal or unusual behaviours, situations, or events in areas dedicated to pedestrian traffic, namely crosswalks, sidewalks, or pedestrian bridges. The main objective is to improve efficiency, safety, and security in the urban environment by identifying deviations and monitoring pedestrian activities from established norms. This kind of AD typically includes surveillance cameras, sensors, and advanced software algorithms. Using advanced machine learning (ML) and computer vision (CV) approaches, this technique continuously monitors the pedestrian area to detect potential threats and irregularities. Deep Learning Assisted AD in Pedestrian Walkways presents a novel and very efficient method to enhance security and safety in urban environments. Therefore, this study designs an Intelligent Multi-Group Marine Predator Algorithm with Deep Learning Assisted Anomaly Detection (MMPADL-AD) in Pedestrian Walkways. The MMPADL-AD system aims to ensure security in PWs via the AD process. The MMPADL-AD technique incorporates a NASNet feature extractor that proficiently extracts high-level features from surveillance data, allowing a deep understanding of pedestrian behaviours. Besides, the MMPADL-AD technique applies convolutional long short-term memory (ConvLSTM), inheriting the benefits of convolutional neural networks) and LSTM for the AD process. Finally, the MMPA has been used for the hyperparameter tuning mechanism, which optimizes the model's performance, assuring accuracy and adaptability. Benchmark data accompanied an extensive set of experiments to ensure the higher effectiveness of the MMPADL-AD approach. The experimental values highlighted the supremacy of the MMPADL-AD approach over other DL methods.

INDEX TERMS Data science, artificial intelligence, intelligent computing, anomaly detection, computer vision.

I. INTRODUCTION

Yearly, 270,000 pedestrians nearly miss their lives on the world's highways. Responding to pedestrian security is integral to the struggle to stop road traffic damage [1]. Pedestrian accidents, such as further road traffic smashes, will not be as familiar as expected because they are avoidable and predictable [2]. Present technologies, including surveillance cameras (CCTV), computer vision (CV), and others, are utilized to protect pedestrians and support security walking, which requires understanding the risk factors for pedestrian smashes. The main goal of this research is to ensure the

The associate editor coordinating the review of this manuscript and approving it for publication was Jolanta Mizera-Pietraszko.

security and safety of PWS by utilizing computer vision models [3]. The surveillance camera in public areas managed the CV-centric technique to absorb the status of the CV study team. The seized visual information comprises enhanced facts that are more correct than the alternative data sources such as radar signals, mobile communication, GPS, and many others [4], [5].

Anomaly detection (AD) is challenging for several reasons; primarily, the description of an anomaly varies from context to context [6]. Next, various options for what creates an anomaly may be unlimited. Then, strange data facts with real-world information tend to lie carefully to what is well-defined as usual. Finally, if anomalies rarely appear, robustness features from the data should be extracted [7]. The above-discussed list will only capture some of the probable reasons that make the problem so hard, but researchers have considered these points in past years while developing novel solutions to the problem. Due to dimensionality swearing, several conventional anomaly recognition models could better demonstrate complex high-dimensional supplies [8]. With the fast growth of Deep Learning (DL), numerous specialists have designed new techniques to integrate them with anomaly recognition. The concept behind this is to accord with AD, which means in the training stage, the method absorbs the distribution features of average data [9]. Once the testing is over, the method recognizes all information that does not fit into the usual class as abnormal data [10].

This study designs an Intelligent Multi-Group Marine Predator Algorithm with Deep Learning Assisted Anomaly Detection (MMPADL-AD) in Pedestrian Walkways. The MMPADL-AD system incorporates a NASNet feature extractor that proficiently extracts high-level features from surveillance data, allowing a deep understanding of pedestrian behaviours. Besides, the MMPADL-AD technique applies convolutional long short-term memory (ConvLSTM), inheriting the benefits of convolutional neural network (CNN) and LSTM for the AD procedure. Finally, the MMPA has been used for the parameter tuning mechanism, which optimizes the model's performance, assuring accuracy and adaptability. An extensive set of experiments were performed on benchmark data to ensure the higher efficiency of the MMPADL-AD technique.

- The MMPADL-AD model effectively extracts high-level features from surveillance data, allowing for deep comprehension of pedestrian behaviours and improving the technique's capacity for interpreting convolutional scenarios.
- Incorporates the merits of CNN and LSTM models for anomaly recognition processes, allowing the method to comprehend spatial and temporal reliabilities in pedestrian movement patterns effectually
- Implement the MMPA technique for hyperparameter optimization, and the model's performance is fine-tuned to ensure heightened accuracy and adaptability, consequently boosting its effectiveness in real-world settings.

II. LITERATURE REVIEW

In [11], an effective technique is proposed to detect abnormal things automatically and focus anomalous things amongst multi-pedestrian crowds through DL and conditional random field (CRF). In the first stage, the pre-processing is executed on removed frames, and then super-pixels are created by utilizing an enhanced divide transform. Then, the objects are separated by employing a CRF. The areas of interest are restricted by applying conditional possibility, and the sequential connection is executed to trace the areas with pedestrian groups and pedestrians with other items. Al Sulaie [12] developed a novel Golden Jackal Optimization with DL-based AD in PWs (GJODL-ADPW) for road traffic security. This study demoralized the Xception model for the real extraction feature procedure. The GJO approach is often used in this research to determine the optimal hyperparameter. At last, the Bi-LSTM network is employed for anomaly recognition reasons.

Pustokhina et al. [13] devised an automated DL-based AD technique in PW (DLADT-PW) for exposed road consumer security. In the first stage, the DLADT-PW method contains pre-processing, which is then used to extract the noise and increase image quality. The Mask-RCNN with the DenseNet model was also mainly applied for the recognition procedure. Ullah et al. [14] developed a new and effective Gaussian kernel-based integration method (GKIM) for irregular object recognition and localization in pedestrian movements. The GKIM combines spatial-temporal features for effectual and robust motion images to capture characteristic and significant information regarding anomalous things. Next, the author proposed a block-based recognition structure by testing a recurrent CRF by employing the features of GKIM.

Sophia and Chitra [15] propose a Panoptic FPN-based AD and Tracking (PFPN-ADT) technique for PWs. The main aim is to distinguish and organize dissimilar variances in pedestrian footpaths, such as skaters, vehicles, etc. The method includes a panoptic segmentation technique and a PFPN, which are utilized for item detection. For object detection, a Compact Bat Algorithm (CBA) with SAE was used for the detection of familiar items. Alsolai et al. [16] project a new SCA with DL-based AD in PW (SCADL-ADPW) system. The developed SCADL-ADPW model recognizes the occurrence of variances in the PW on RSIs. To achieve this, the SCADL-ADPW model employs the VGG16 method for the feature vector group. The SCA technique was also mainly intended for the optimum parameter tuning procedure. The LSTM method can be exploited for AD.

García-Aguilar et al. [17] developed advanced technology using pre-trained super-resolution (SR) and CNN techniques. This method is divided into two portions. Offline, the pre-tested CNN method estimated a massive dataset of city series to identify and start the common sites of interest parts. Zeng et al. [18] designed a Hierarchical spatiotemporal graph CNN (HSTGCNN) model. Chopra et al. [19] introduce an effectual watermarking model employing a map-based security key via exclusive-OR operation. In [20], an unsupervised

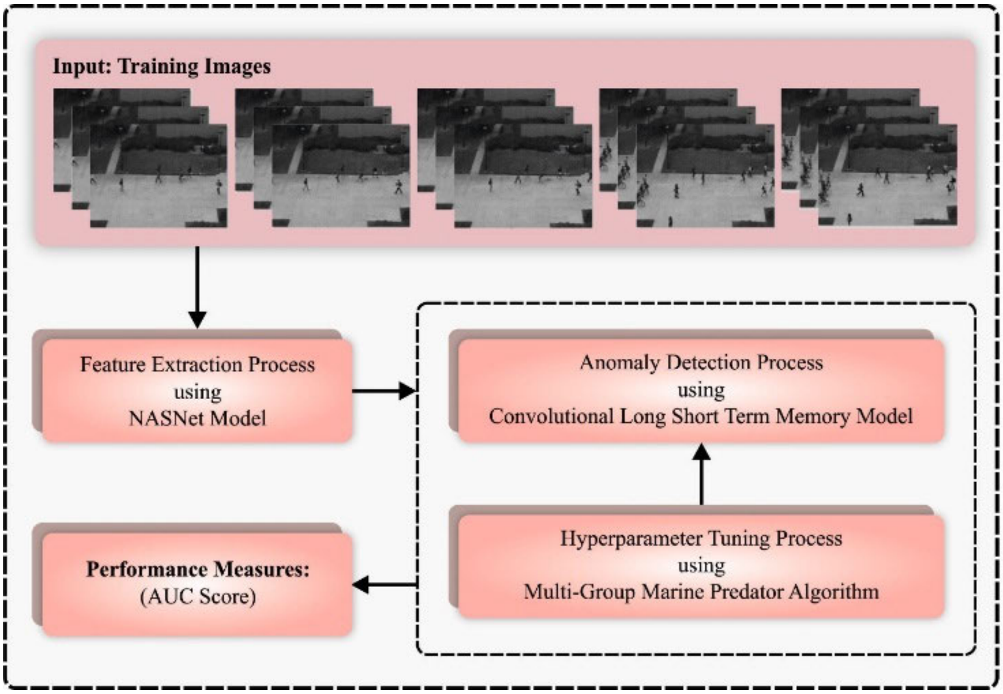

FIGURE 1. The overall process of the MMPADL-AD algorithm.

DL and nearest neighbour classification model is presented, which comprises deblurring with DeblurGAN-v2, semantic segmentation with a hybrid CNN-VIT model, multiscale feature aggregation with an attentional feature fusion module, and K-nearest neighbour classification using pre-trained features.

III. THE PROPOSED MODEL

This article has established an automated AD using the MMPADL-AD method for security in PWs. The MMPADL-AD technique analyses the surveillance videos to ensure security in PWs via the AD process. The MMPADL-AD technique incorporates a NASNet feature extractor, ConvLSTM classifier, and MMPA-based hyperparameter optimizer. Fig. 1 depicts the entire procedure of the MMPADL-AD methodology.

A. FEATURE EXTRACTOR: NASNET MODEL

At this stage, the NASNet approach extracts the features from the surveillance video frames. There is considerable progress in DL and computer vision [21]. It is well-known for its capability to optimize and discover NN architecture automatically for feature extraction, enabling it to capture complicated representations and patterns in visual information effectively. NASNet works based on a neural architecture search (NAS) model that automates designing NNs, saving engineers and researchers considerable effort and time. At the core of NASNet's power is its capability to select and search for optimum NN cell architecture. This process includes exploring different combinations of skip-connection, convolutional, and pooling operations to create NN cells. NASNet detects architecture that achieves better outcomes on a given task through evolutionary or reinforcement learning algorithms. Once these optimum cells are detected, they are stacked to construct robust DNNs personalized for feature extraction. The feature extractor could effectively capture abstract and hierarchical features from the images or other visual information. NASNet has shown remarkable performance on different CV tasks, including object detection and image classification, which outperform manually designed architecture. This makes NASNet an invaluable mechanism for a DL practitioner, as it streamlines the procedure of network design and allows the extraction of discriminative and meaningful features from images, benefiting applications such as AD, image recognition, etc.

B. DETECTION MODULE: CONVLSTM

The ConvLSTM model is applied for classification, which inherits the benefits of CNN and LSTM. LSTM network is a kind of RNN commonly known for addressing drawbacks of long-term memory and processing the data sequence of typical RNN [22]. LSTM lengthens the RNN model using a separate memory unit and gate module controlling the network's data flow. The gate mechanism includes input, forgot, and output gates. This gate controls the data flow throughout the network to enable which data will persist from the memory cell. LSTM network can preserve essential data and remove irrelevant data. Then, to differentiate independent memory cells from hidden state h_t in LSTM, it is signified as c_t. The forget gate f_t attains input x_t and h_{t-1} to decide that data should be maintained in c_{t-1}. The activation function, 0_t, and f_t gates are sigmoid layers where all the values are projected within [0,1], whereas c_{t-1} provides the data retention to define the scale. The abovementioned processes are defined formally by using the following expression:

$$i_t = \sigma\left(W_{xi}x_t + W_{hi}h_{t-1} + W_{ci}c_{t-1} + b_i\right) \quad (1)$$

$$f_t = \sigma\left(W_{xf}x_t + W_{hf}h_{t-1} + W_{cf}c_{t-1} + b_f\right) \quad (2)$$

$$O_t = \sigma\left(W_{xo}x_t + W_{ho}h_{t-1} + W_{co}c_t + b_o\right) \quad (3)$$

$$c_t = f_t c_{t-1} + i_t \emptyset\left(W_{xc}x_t + W_{hc}h_{t-1} + b_c\right) \quad (4)$$

$$h_t = O_t \emptyset\left(c_t\right) \quad (5)$$

$W_{xi}, W_{hi}, W_{ci}, W_{xf}, W_{hf}, W_{cf}, W_{xo}, W_{ho}, W_{co}, W_{xc}$, and W_{hc} are the weight matrices for the gates and cell state memory. The bias of gates is denoted as b_i, bo, b_f, and b_c while representing an entry-wise multiplication process. c_t is a cell state, and h_{t-1} is a prior hidden state. Likewise $\emptyset$, it shows a hyperbolic tangent function, and σ represents the logistic sigmoid function. Eqs. (6) & (7) shows the activation functions:

$$\sigma(x) = \frac{1}{1+e^{-x}} \quad (6)$$

$$\emptyset(x) = \frac{e^x - e^{-x}}{e^x + e^{-x}} \quad (7)$$

Learning via the FC layer of LSTM has proved effective in handling temporal relations, but a redundancy from spatial information has made it increasingly difficult. The whole connection LSTM has added an extension having convolution assembly in input-to-state transition and state-to-state transition to address these challenges. By forecasting mechanisms and forming encoding, stacking multiple layers of ConvLSTM has made the network incapable of spatiotemporal forecasting and precipitation new casting. Like the classical full connection LSTM, ConvLSTM is essential for dealing with more complicated sequences. This layer acts as an encoder that encodes the input-refined series with a definite size later transmitted to LSTM. ConvLSTM employs convolution operations for hidden-hidden and input-hidden connections.

Fig. 2 illustrates the architecture of ConvLSTM. The ConvLSTM layer with convolution operation is used to replace matrix multiplication operation in RNN, and this layer can be used to know which data should be forgotten or retained from the prior cell state. Likewise, ConvLSTM decides which data needs to be stored in the existing cells. The ConvLSTM model can be defined in Eqs (12) to (16). After ConvLSTM, other LSTM layers are plugged in to learn the feature maps and provide the last prediction. This hybrid connection makes it more effective and efficient concerning image classification:

$$i_t = \sigma\left(W_{xi} * x_t + W_{hi} * h_{t-1} + W_{ci}{}^{\circ} c_{t-1} + b_i\right) \quad (8)$$

$$f_t = \sigma\left(W_{xf} * x_t + W_{hf} * h_{t-1} + W_{cf} \circ c_{t-1} + b_f\right) \quad (9)$$

$$O_t = \sigma\left(W_{xo} * x_t + W_{ho} * h_{t-1} + W_{co} \circ c_t + b_o\right) \quad (10)$$

$$c_t = f_t c_{t-1} + i_t \emptyset\left(W_{xc} * x_t + W * h + b_c\right) \quad (11)$$

$$h_t = O_t \otimes \left(c_t\right) \quad (12)$$

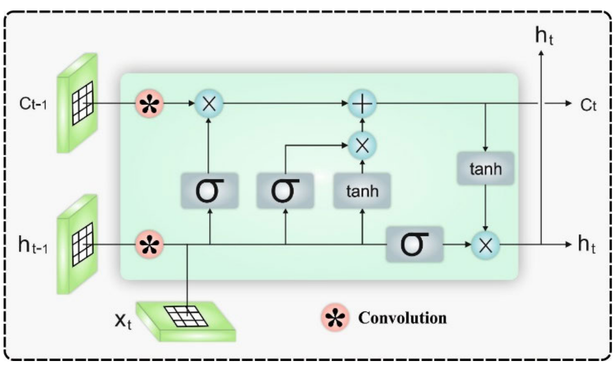

FIGURE 2. Structure of ConvLSTM.

C. HYPERPARAMETER TUNING: MMPA

Lastly, the MMPA adjust the hyperparameter value of the ConvLSTM model. MPA is a new optimization algorithm that draws inspiration from predator and prey behaviours while searching for food [23]. MPA is simple and easy to implement. It has good performance in optimization problems. However, it prematurely converges due to an imbalance in its exploitation and exploration abilities. The study proposes an MMPA to optimize the MPA performance. The multi-group process splits the original population into various groups. This group creates an Elite matrix and top predator using communication information and multiple strategies.

The multi-group mechanism splits the population into various groups, which produces the top predator using different strategies. The proposed MMPA might achieve collaborative work throughout groups and optimize the use of each performance through a multi-group process and producing approach.

Accordingly, the top predator is critical to the optimizer technique. The top predator is used to construct an Elite matrix as part of the optimizer algorithm to discover food. This will recommend four producing approaches to create the top predator and Elite matrix to enhance the performance of MMA further.

1) GENERATION METHOD 1

The optimum outcomes of a group of people. During the optimization procedure, if the parameters related to the outcomes are autonomous, it is easy to generate the best solutions by interchanging knowledge inside the identical group. Where $itr = oS$ iteration $(0 = 1, 2, 3 \ldots)$, the optimum outcomes $y_{best,h}(u)$ of the similar group generates an Elite matrix in strategy 1.

$$y_{best,h}(u) = Best\left\{y_{1,h}(u), y_{2,h}(u), \ldots, y_{o,h}(u)\right\}. \quad (13)$$

In Eq. (13), $y_{1,h}(u), y_{2,h}(u), \ldots, y_{o,h}(u)$ represent the h^{th} group's o solutions.

2) GENERATION METHOD 2

The average of a similar group's solution. The control of method 2 is identical to method 1. In strategy 2, when $itr = oS$ iteration $(o = 1, 2, 3 \ldots)$, then average performance $y_{avg,h}(u)$ is generated by averaging l suitable method of the identical group for the diversity of the population. The $y_{avg,h}(u)$ is used to make the Elite matrix,

$$y_{avg,h}(u) = \frac{y_{1,h}(u), y_{2,h}(u), \ldots, y_{o,h}(u)}{l}. \tag{14}$$

In Eq. (14), $y_{1,h}(u), y_{2,h}(u), \ldots, y_{o,h}(u)$ is the l appropriate solution of h^{th} groups.

3) GENERATION METHOD 3

The whole group's optimum technique. During the optimization process, if the parameter related to the solution is weakly connected, it leads to the best solutions by interchanging data among each group. Where $itr = oS$ iteration $(0 = 1, 2, 3 \ldots)$ is applied in method 3, the optimum option $y_{\max}(u)$ of complete groups is utilized to generate the Elite matrix.

$$y_{\max}(u) = Best\{y_1(u), y_2(u), \ldots, y_0(u)\}, \tag{15}$$

$y_1(u), y_2(u), \cdots, y_0(u)$ is the O solution in the entire group.

4) GENERATION METHOD 4

The average of whole groups' performances. The impact of method 4 is similar to that of method 3. In strategy 4, when $itr = oS$ iteration $(o = 1, 2, 3 \ldots)$, the average solution $y_{avg}(u)$ is calculated by summing the optimum solution of all the groups for population diversity. $ploy y_{avg}(u)$ is used to make the Elite matrix.

$$y_{avg}(u) = \frac{y_{\max,1}(u), y_{\max,2}(u), y_{\max,3}(u), \ldots, y_{\max,H}(u)}{H}. \tag{16}$$

In Eq. (16), the letter H refers to the total number of groups. $y_{\max,1}(u), y_{\max,2}(u), y_{\max,3}(u), \ldots, y_{\max,H}(u)$ is the best outcome of all the groups.

The fitness choice is a primary factor in the MMPA technique. The encoded results have been exploited to assess the goodness of the performance candidates. The accuracy values are the primary condition used to design an FF.

$$Fitness = \max(P) \tag{17}$$

$$P = \frac{TP}{TP + FP} \tag{18}$$

Meanwhile, TP and FP are true positive and false positive values.

IV. RESULTS AND DISCUSSION

The anomaly detection outcome of the MMPADL-AD system is tested on three datasets: UCSDPed1, UCSDPed2, and Avenue datasets, as represented in Table 1.

To computer the efficiency of the MMPADL-AD technique on the UCSDPed1 dataset, we have created $accu_y$ curves for training (TR) as well as testing (TS) stages, as illustrated in Fig. 3. These curves deliver an appreciated understanding of the technique's learning growth and its capability to generalize. However, as the number of epochs rises, an observable development in TR and TS $accu_y$ curves becomes apparent. This improvement designates the model's ability to improve and identify designs in both datasets.

Fig. 4 also outlines the MMPADL-AD technique loss values under the TR procedure on the UCSDPed1 dataset. The decreasing trend in TR loss with epochs specifies that the

TABLE 1. Details on database.

Dataset	No. of Videos	Training Set	Testing Set	Average Frames	Dataset Length
UCSDPed1 (Bikers, small carts, walking across walkways)	70	34	36	201	5 min
UCSDPed2 (Bikers, small carts, walking across walkways	28	16	12	163	5 min
Avenue (Run, throw, new object)	37	16	21	839	5 min

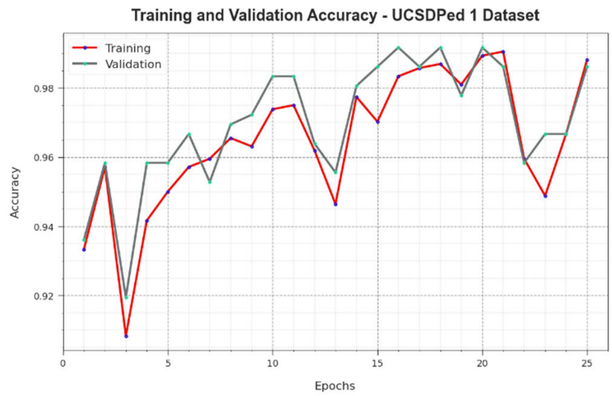

FIGURE 3. $Accu_y$ **curve of MMPADL-AD algorithm on UCSDPed1 dataset.**

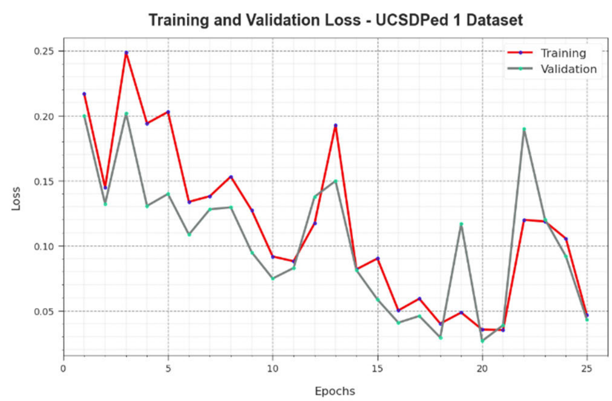

FIGURE 4. Loss curve of MMPADL-AD algorithm on UCSDPed1 dataset.

method repeatedly refines its weights to decrease prediction errors on both databases. This loss curve replicates how well the technique fits the TR data. Notably, the TR and TS loss constantly drop, validating the method's effectual learning of designs obtainable in both TR and TTS data. In addition, it displays the model's version in decreasing differences among predictive and novel TR labels.

Table 2 and Fig. 5 represent the TPR outcomes of the MMPADL-AD method on the UCSDPed1 dataset [24]. The outcomes signify that the SF and MPPCA algorithms are depicted as the lowest outcome. At the same time, the EADN and AMDN models have managed to report moderate performance. Meanwhile, the ADPW-FLHHO model has tried to accomplish considerable outcomes. However, the MMPADL-AD technique reaches maximum TPR performance over varying FPR rates.

TABLE 2. TPR outcome of MMPADL-AD algorithm with other systems on UCSDPed1 database.

TPR						
FPR	MPPCA	SF	AMDN	EADN	ADPW-FLHHO	MMPADL-AD
0	0.0000	0.0000	0.0000	0.0000	0.0000	0.0000
5	0.0920	0.1318	0.3256	0.3468	0.5962	0.7136
10	0.2274	0.2459	0.4478	0.5508	0.7446	0.8612
15	0.3522	0.3681	0.5669	0.7555	0.8244	0.8923
20	0.4318	0.4583	0.6997	0.7551	0.8749	0.9309
25	0.5191	0.5356	0.6837	0.7380	0.9382	0.9525
30	0.5749	0.6331	0.8480	0.9438	0.9621	0.9776
35	0.6359	0.7182	0.9064	0.9568	0.9726	0.9879
40	0.6810	0.8109	0.9278	0.9648	0.9783	0.9890
45	0.7552	0.8825	0.9409	0.9727	0.9836	0.9908
50	0.7977	0.9093	0.9621	0.9780	0.9863	0.9953
55	0.8324	0.9330	0.9727	0.9781	0.9862	0.9983
60	0.8801	0.9411	0.9781	0.9781	0.9886	1.0000
65	0.9118	0.9488	0.9808	0.9836	0.9886	1.0000
70	0.9541	0.9570	0.9807	0.9833	1.0000	1.0000
75	0.9568	0.9756	0.9836	0.9885	1.0000	1.0000
80	0.9623	0.9833	1.0000	1.0000	1.0000	1.0000
85	0.9674	0.9835	1.0000	1.0000	1.0000	1.0000
90	0.9835	0.9834	1.0000	1.0000	1.0000	1.0000
95	0.9808	0.9939	1.0000	1.0000	1.0000	1.0000
100	1.0000	1.0000	1.0000	1.0000	1.0000	1.0000

Fig. 6 illustrates the comparative AUC_{score} results of the MMPADL-AD technique. The obtained values of the

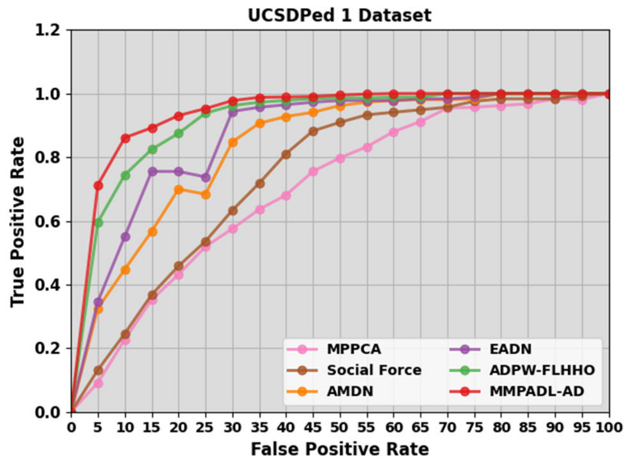

FIGURE 5. TPR outcome of MMPADL-AD algorithm on UCSDPed1 dataset.

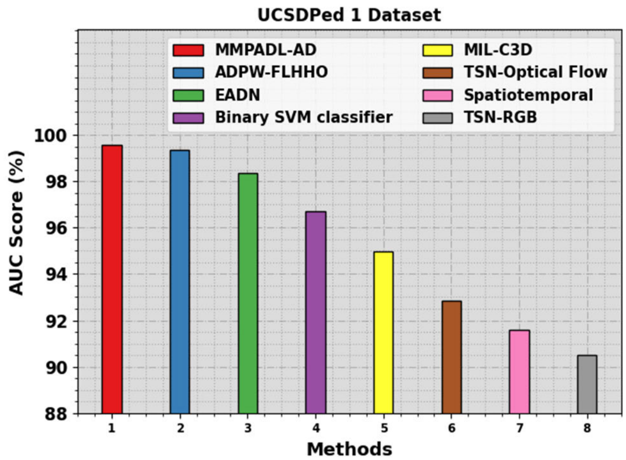

FIGURE 6. AUC_{score} outcome of MMPADL-AD approach under UCSDPed1 dataset.

MMPADL-AD technique accomplish an enhanced AUC_{score} of 99.57%. On the other hand, the ADPW-FLHHO, EADN, binary SVM, MIL-C3D, TSN-Optical Flow, Spatiotemporal, and TSN-RGB approaches obtain decreased AUC_{score} values of 99.36%, 98.36%, 96.73%, 94.99%, 92.86%, 91.57%, and 90.49%, respectively.

For computing the effectiveness of the MMPADL-AD approach on the UCSDPed2 dataset, we have produced $accu_y$ curves for the TR and TS sets, as illustrated in Fig. 7. These curves provide valuable perceptions into the model's learning development and its capacity to simplify. Since it increases the epoch numbers, a perceptible development in TR and TS $accu_y$ curves becomes evident. This growth shows the model's ability to improve and distinguish patterns from TR and TS datasets.

Fig. 8 also summarises the MMPADL-AD methodology loss values during the TR procedure on the UCSDPed2 dataset. The decreasing trend in TR loss over epochs shows that the approach frequently improves weights to diminish prediction errors on both databases. This loss curve

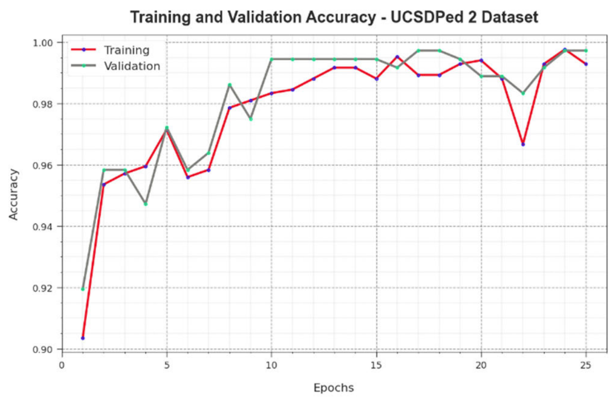

FIGURE 7. $Accu_y$ **curve of MMPADL-AD system under UCSDPed2 dataset.**

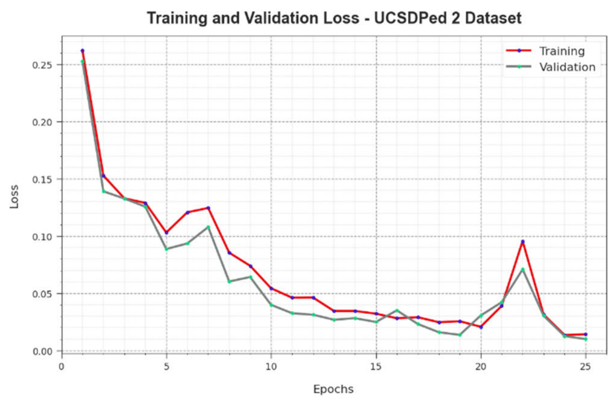

FIGURE 8. Loss curve of MMPADL-AD method on UCSDPed2 database.

reproduces how well the technique fits the TR data. Significantly, the TR and TS loss dependably decrease, validating the model's effective design learning in both data. Moreover, it expresses the model's version by diminishing differences among predictive and new TR labels.

Table 3 and Fig. 9 represent the TPR outcomes of the MMPADL-AD model on the UCSDPed2 database. The

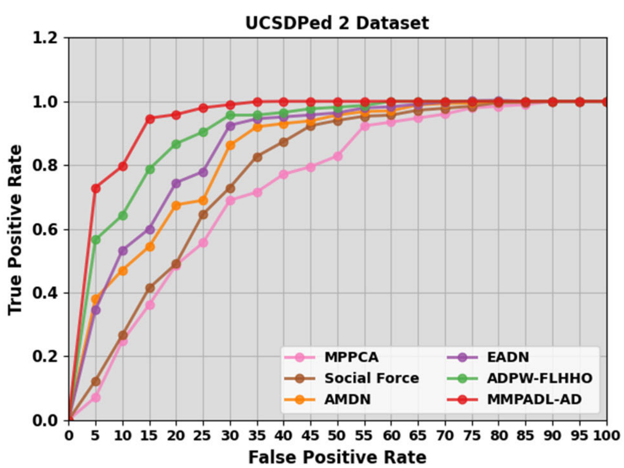

FIGURE 9. TPR outcome of MMPADL-AD method on UCSDPed2 dataset.

TABLE 3. TPR outcome of MMPADL-AD algorithm with other methodologies under UCSDPed2 database.

TPR						
FPR	MPPCA	SF	AMDN	EADN	ADPW-FLHHO	MMPADL-AD
0	0.0000	0.0000	0.0000	0.0000	0.0000	0.0000
5	0.0718	0.1237	0.3800	0.3455	0.5654	0.7294
10	0.2474	0.2661	0.4704	0.5326	0.6423	0.7963
15	0.3615	0.4140	0.5441	0.5998	0.7870	0.9470
20	0.4861	0.4903	0.6751	0.7448	0.8671	0.9586
25	0.5560	0.6456	0.6895	0.7792	0.9038	0.9796
30	0.6892	0.7292	0.8621	0.9248	0.9567	0.9895
35	0.7149	0.8268	0.9199	0.9450	0.9567	0.9989
40	0.7711	0.8734	0.9303	0.9512	0.9653	1.0000
45	0.7947	0.9232	0.9386	0.9571	0.9767	1.0000
50	0.8283	0.9400	0.9568	0.9640	0.9815	1.0000
55	0.9229	0.9532	0.9679	0.9791	0.9870	1.0000
60	0.9347	0.9566	0.9702	0.9828	1.0000	1.0000
65	0.9476	0.9722	0.9885	0.9910	1.0000	1.0000
70	0.9599	0.9782	0.9929	0.9974	1.0000	1.0000
75	0.9792	0.9848	0.9947	1.0017	1.0000	1.0000
80	0.9848	0.9958	1.0003	1.0031	1.0000	1.0000
85	0.9897	0.9973	1.0000	1.0000	1.0000	1.0000
90	1.0000	1.0000	1.0000	1.0000	1.0000	1.0000
95	1.0000	1.0000	1.0000	1.0000	1.0000	1.0000
100	1.0000	1.0000	1.0000	1.0000	1.0000	1.0000

outcome implied that the SF and MPPCA techniques have shown the least performance. Similarly, the EADN and AMDN methods have achieved moderate performance. Meanwhile, the ADPW-FLHHO technique has tried to achieve significant outcomes. However, the MMPADL-AD model reaches extreme TPR performance over varying FPR rates.

Fig. 10 explains a comparative AUC_{score} outcome of the MMPADL-AD model. The achieved values of the MMPADL-AD method resulted in an improved AUC_{score} of 99.36%. In addition, the ADPW-FLHHO, EADN, binary SVM, MIL-C3D, TSN-Optical Flow, Spatiotemporal, and TSN-RGB approaches attain diminished AUC_{score} values of 99.19%, 98.30%, 97.16%, 95.50%, 94.36%, 92.48%, and 90.44%, correspondingly.

To compute the efficiency of the MMPADL-AD approach on the Avenue dataset, we have created $accu_y$ curves for

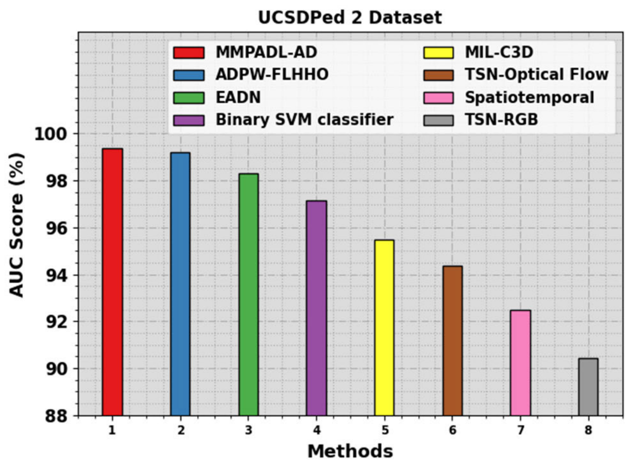

FIGURE 10. AUC_{score} outcome of MMPADL-AD algorithm on UCSDPed2 dataset.

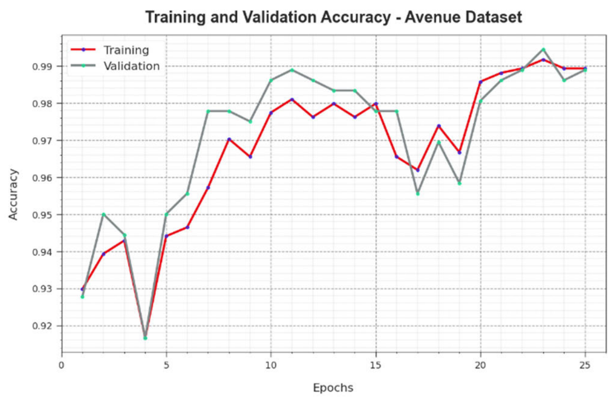

FIGURE 11. $Accu_y$ curve of MMPADL-AD algorithm on Avenue dataset.

FIGURE 12. Loss curve of MMPADL-AD algorithm on Avenue dataset.

the TR and TS sets, as illustrated in Fig. 11. These curves provide an appreciated understanding of the model's learning growth and its capacity to simplify. However, it can increase the number of epochs, and a clear development in TR and TS $accu_y$ curves becomes evident. This development implies the technique's better ability to distinguish designs from both datasets.

Fig. 12 also offers an overview of the MMPADL-AD technique loss values during the TR procedure on the Avenue dataset. The lesser development in TR loss with epochs designates that the methodology frequently refines its weights to decrease forecast errors on both databases. This loss curve imitates how well the method fits the TR data. Mainly, the TR and TS losses are regularly lesser, specifying that the model is productive patterns learning in both data. Additionally, it displays the model's variation in minimizing differences between predictive and new TR labels.

Table 4 and Fig. 13 denote the TPR outcome of the MMPADL-AD approach on the Avenue database. The performance depicts that the SF and MPPCA techniques have shown the most minor performance. At the same time, the EADN and AMDN models have accomplished reported moderate results. Meanwhile, the ADPW-FLHHO approach

TABLE 4. TPR outcome of MMPADL-AD algorithm with other systems on Avenue database.

TPR						
FPR	MPPCA	SF	AMDN	EADN	ADPW-FLHHO	MMPADL-AD
0	0.0000	0.0000	0.0000	0.0000	0.0000	0.0000
5	0.1100	0.1858	0.3308	0.3421	0.5710	0.7310
10	0.2489	0.2948	0.4609	0.5545	0.5867	0.7377
15	0.3245	0.4189	0.5935	0.5975	0.7399	0.9079
20	0.4646	0.4516	0.6895	0.7270	0.8667	0.9399
25	0.6041	0.6538	0.7288	0.7400	0.8882	0.9556
30	0.6407	0.7704	0.8889	0.9231	0.9484	0.9699
35	0.7116	0.7897	0.9037	0.9514	0.9594	0.9859
40	0.7845	0.8608	0.9254	0.9752	0.9612	0.9892
45	0.8314	0.9296	0.9729	0.9789	0.9731	0.9989
50	0.8324	0.9370	0.9744	0.9843	0.9834	1.0000
55	0.8830	0.9428	0.9805	0.9872	0.9873	1.0000
60	0.9011	0.9546	0.9951	0.9931	0.9954	1.0000
65	0.9463	0.9617	0.9961	0.9978	1.0000	1.0000
70	0.9568	0.9659	0.9971	1.0000	1.0000	1.0000
75	0.9663	0.9899	0.9985	1.0000	1.0000	1.0000
80	0.9740	1.0000	1.0000	1.0000	1.0000	1.0000
85	0.9809	1.0000	1.0000	1.0000	1.0000	1.0000
90	1.0000	1.0000	1.0000	1.0000	1.0000	1.0000
95	1.0000	1.0000	1.0000	1.0000	1.0000	1.0000
100	1.0000	1.0000	1.0000	1.0000	1.0000	1.0000

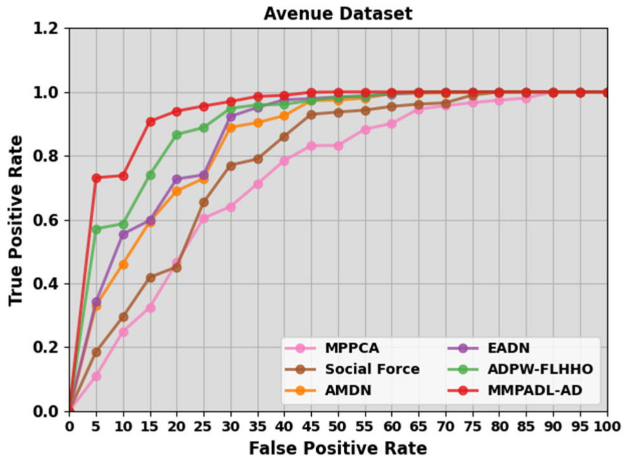

FIGURE 13. TPR outcome of MMPADL-AD algorithm on Avenue dataset.

has tried to achieve considerable results. However, the MMPADL-AD method attains determined TPR performance over varying FPR rates.

Fig. 14 shows a comparative AUC_{score} outcome of the MMPADL-AD model. The attained values of the MMPADL-AD model accomplish a greater AUC_{score} of 99.05%. On the other hand, the ADPW-FLHHO, EADN, binary SVM, MIL-C3D, TSN-Optical Flow, Spatiotemporal, and TSN-RGB techniques acquire reduced AUC_{score} values of 98.90%, 97.78%, 96.21%, 95.02%, 93.31%, 91.41%, and 89.47%, correspondingly.

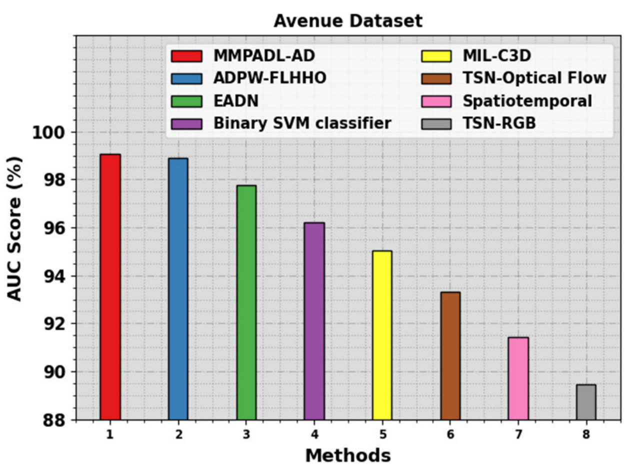

FIGURE 14. AUC_{score} outcome of MMPADL-AD system on Avenue dataset.

These results show the practical ability of the MMPADL-AD methodology in anomaly detection.

V. CONCLUSION

This article has established an automated AD using the MMPADL-AD method for security in PWs. The MMPADL-AD technique analyses the surveillance videos to ensure security in PWs via the AD process. The MMPADL-AD technique incorporates a NASNet feature extractor, ConvLSTM classifier, and MMPA-based hyperparameter optimizer. The NASNet feature extractor enables the derivation of high-level features from surveillance data, allowing a deep understanding of pedestrian behaviours. The ConvLSTM model is applied for classification, which inherits the benefits of CNN and LSTM. Lastly, the MMPA is used for the hyperparameter tuning mechanism, which optimizes the model's performance, assuring accuracy and adaptability. Benchmark data accompanied an extensive set of experiments to ensure the higher efficiency of the MMPADL-AD method. The simulation values highlighted the supremacy of the MMPADL-AD method with other DL methodologies. The efficiency of the MMPADL-AD method may be restricted in highly crowded or dynamic pedestrian environments. Future studies may focus on improving the robustness of the model to several environmental conditions.

ACKNOWLEDGMENT

The authors would like to acknowledge and thank for the support from Ajman University, United Arab Emirates.

REFERENCES

[1] Y. Luo, C. Zhang, M. Zhao, H. Zhou, and J. Sun, "Where, what, whether: Multimodal learning meets pedestrian detection," in *Proc. IEEE/CVF Conf. Comput. Vis. Pattern Recognit.*, Jun. 2020, pp. 14065–14073.

[2] Y. Zhu, J. Yang, X. Xieg, Z. Wang, and X. Deng, "Long-distanceinfrared video pedestrian detection using deep learning and backgroundsubtraction," *J. Phys., Conf.*, vol. 1682, no. 1, Nov. 2020, Art. no. 012012.

[3] D. Guan, Y. Cao, J. Yang, Y. Cao, and M. Y. Yang, "Fusion of multispectral data through illumination-aware deep neural networks for pedestrian detection," *Inf. Fusion*, vol. 50, pp. 148–157, Oct. 2019.

[4] B. Kim, N. Yuvaraj, K. R. Sri Preethaa, R. Santhosh, and A. Sabari, "Enhanced pedestrian detection using optimized deep convolution neural network for smart building surveillance," *Soft Comput.*, vol. 24, no. 22, pp. 17081–17092, Nov. 2020.

[5] K. Dasgupta, A. Das, S. Das, U. Bhattacharya, and S. Yogamani, "Spatio-contextual deep network-based multimodal pedestrian detection for autonomous driving," *IEEE Trans. Intell. Transp. Syst.*, vol. 23, no. 9, pp. 15940–15950, Sep. 2022.

[6] S. Liu, D. Huang, and Y. Wang, "Adaptive NMS: Refining pedestrian detection in a crowd," in *Proc. IEEE/CVF Conf. Comput. Vis. Pattern Recognit. (CVPR)*, Jun. 2019, pp. 6452–6461.

[7] M. Aledhari, R. Razzak, R. M. Parizi, and G. Srivastava, "Multimodal machine learning for pedestrian detection," in *Proc. IEEE 93rd Veh. Technol. Conf. (VTC-Spring)*, Apr. 2021, pp. 1–7.

[8] Y. Pang, J. Xie, M. H. Khan, R. M. Anwer, F. S. Khan, and L. Shao, "Mask-guided attention network for occluded pedestrian detection," in *Proc. IEEE/CVF Int. Conf. Comput. Vis. (ICCV)*, Oct. 2019, pp. 4966–4974.

[9] D. Yan, C. Shi, T. Li, and Y. Li, "FlexPDR: Fully flexible pedestrian dead reckoning using online multimode recognition and time-series decomposition," *IEEE Internet Things J.*, vol. 9, no. 16, pp. 15240–15254, Aug. 2022.

[10] A. Wolpert, M. Teutsch, M. S. Sarfraz, and R. Stiefelhagen, "Anchor-free small-scale multispectral pedestrian detection," 2020, *arXiv:2008.08418*.

[11] F. Abdullah and A. Jalal, "Multi-pedestrians anomaly detection via conditional random field and deep learning," in *Proc. 4th Int. Conf. Advancements Comput. Sci. (ICACS)*, Feb. 2023, pp. 1–6.

[12] S. Al Sulaie, "Golden jackal optimization with deep learning-based anomaly detection in pedestrian walkways for road traffic safety," in *Proc. Int. Conf. Innov. Comput. Commun.*, Singapore: Springer, Feb. 2023, pp. 617–636.

[13] I. V. Pustokhina, D. A. Pustokhin, T. Vaiyapuri, D. Gupta, S. Kumar, and K. Shankar, "An automated deep learning based anomaly detection in pedestrian walkways for vulnerable road users safety," *Saf. Sci.*, vol. 142, Oct. 2021, Art. no. 105356.

[14] H. Ullah, A. B. Altamimi, M. Uzair, and M. Ullah, "Anomalous entities detection and localization in pedestrian flows," *Neurocomputing*, vol. 290, pp. 74–86, May 2018.
[15] B. Sophia and D. Chitra, "Segmentation based real time anomaly detection and tracking model for pedestrian walkways," *Intell. Autom. Soft Comput.*, vol. 36, no. 3, pp. 2491–2504, 2023.
[16] H. Alsolai, F. N. Al-Wesabi, A. Motwakel, and S. Drar, "Assisting visually impaired people using deep learning-based anomaly detection in pedestrian walkways for intelligent transportation systems on remote sensing images," *J. Disability Res.*, vol. 2, no. 2, pp. 49–56, 2023.
[17] I. García-Aguilar, R. M. Luque-Baena, E. Domínguez, and E. López-Rubio, "Small-scale urban object anomaly detection using convolutional neural networks with probability estimation," *Sensors*, vol. 23, no. 16, p. 7185, Aug. 2023.
[18] X. Zeng, Y. Jiang, W. Ding, H. Li, Y. Hao, and Z. Qiu, "A hierarchical spatio-temporal graph convolutional neural network for anomaly detection in videos," *IEEE Trans. Circuits Syst. Video Technol.*, vol. 33, no. 1, pp. 200–212, Jan. 2023.
[19] J. Chopra, A. Kumar, A. K. Aggarwal, and A. Marwaha, "An efficient watermarking for protecting signature biometric template," in *Proc. 5th Int. Conf. Signal Process. Integr. Netw. (SPIN)*, Feb. 2018, pp. 413–418.
[20] N. Guo, C. Lin, H. Yan, J. Zang, and M. Xiong, "Real-time pantograph anomaly detection using unsupervised deep learning and K-nearest neighbor classification," *IEEE Trans. Instrum. Meas.*, vol. 73, pp. 1–13, 2024.
[21] C. Yu, X. Liu, W. Feng, C. Tang, and J. Lv, "GPT-NAS: Evolutionary neural architecture search with the generative pre-trained model," 2023, *arXiv:2305.05351*.
[22] N. Khan, I. U. Haq, F. U. M. Ullah, S. U. Khan, and M. Y. Lee, "CL-Net: ConvLSTM-based hybrid architecture for batteries' state of health and power consumption forecasting," *Mathematics*, vol. 9, no. 24, p. 3326, Dec. 2021.
[23] G. Krithiga and V. Mohan, "Elimination of harmonics in multilevel inverter using multi-group marine predator algorithm-based enhanced RNN," *Int. Trans. Electr. Energy Syst.*, vol. 2022, pp. 1–13, Jun. 2022.
[24] M. A. Alohali, M. Aljebreen, N. Nemri, R. Allafi, M. A. Duhayyim, M. I. Alsaid, A. A. Alneil, and A. E. Osman, "Anomaly detection in pedestrian walkways for intelligent transportation system using federated learning and Harris hawks optimizer on remote sensing images," *Remote Sens.*, vol. 15, no. 12, p. 3092, Jun. 2023, doi: 10.3390/rs15123092.